Relativistic Coulomb excitation around grazing impact parameters

B. F. Bayman
School of Physics, Astronomy, University of Minnesota, 116 Church Street S.E., Minneapolis, Minnesota 55455, USA

F. Zardi
Istituto Nazionale di Fisica Nucleare, Dipartimento di Fisica, Via Marzolo, 8 I-35131 Padova, Italy

(Received 18 May 2006; published 17 August 2006)

The semiclassical model of relativistic Coulomb excitation is studied in situations in which the impact parameter is small enough so that projectile and target charge distributions overlap. The electromagnetic effects of this overlap are shown to be small. Realistic nucleon-nucleon reaction cross sections and realistic nuclear radial charge and matter distributions are used to determine a formula for the lower impact parameter limit to be used in the calculation of the Coulomb excitation cross section. A wide selection of projectile-target pairs is explored, in the bombarding energy range of 1 to 5 GeV per nucleon.

DOI: 10.1103/PhysRevC.74.024905 PACS number(s): 25.70.De, 25.75.−q, 24.30.Cz

I. INTRODUCTION

The semiclassical approach to relativistic Coulomb excitation (RCE) assumes that the Coulomb impulse suffered by the projectile nucleus as it passes the target nucleus is small compared to the linear momentum of the projectile. Then the deflection of the projectile will be small, and its trajectory can be approximated by a straight line, with impact parameter b. If b is large enough so that the projectile and target do not experience each other's nuclear forces, the only processes that can occur are electromagnetic. For example, as the projectile moves along its trajectory, the electromagnetic fields it produces can induce transitions in the target.[1] The RCE cross section for the population of a final target state ψ_α, starting with the target ground state $\psi_{\text{g.s.}}$, is given by

$$\sigma_{\text{g.s.}\to\alpha} = 2\pi \int_{b=b_{\min}}^{\infty} b\, db P_{\text{g.s.}\to\alpha}(b), \tag{1.1}$$

where $P_{\text{g.s.}\to\alpha}(b)$ is the probability of the $\psi_{\text{g.s.}} \to \psi_\alpha$ target transition when the target experiences the electromagnetic impulse due to the projectile following an orbit with impact parameter b.

The choice of $b_{\min}$ can have a significant effect on $\sigma_{\text{g.s.}\to\alpha}$ calculated with Eq. (1.1), since $P_{\text{g.s.}\to\alpha}(b)$ has its greatest value at $b = b_{\min}$. This is because the projectile electromagnetic fields at the target are greatest when the two are in closest proximity. Also, for small b, the electromagnetic impulse at the target is more sudden, which makes it more effective at exciting high-energy target states, such as giant multipole excitations. One of the goals of this paper is to provide reliable values of $b_{\min}$ for a wide variety of projectile-target pairs and a wide range of relativistic bombarding energies.

The assumption behind Eq. (1.1) is that there are no nuclear interactions when $b \geqslant b_{\min}$; but when $b < b_{\min}$, the nuclear interactions are so strong that they dominate over electromagnetic processes, and we no longer have Coulomb excitation. We will refer to this latter situation using the term *absorption*. A more realistic discussion would involve a continuous transition as b increases, from complete absorption at small b to zero absorption at large b. If $X(b)$ is the probability that a projectile traverses its orbit with no nuclear interaction with the target, the absorption probability would be $1 - X(b)$, and the RCE cross section would be

$$\sigma_{\text{g.s.}\to\alpha} = 2\pi \int_{b=0}^{\infty} b\, db P_{\text{g.s.}\to\alpha}(b) \times X(b). \tag{1.2}$$

The function $X(b)$ can be estimated by folding the nuclear density distributions of the projectile and target with the nucleon-nucleon interaction cross section.

For the small-b range of the integral in Eq. (1.2), there are situations in which the tails of the projectile and target overlap. When this happens, the electromagnetic interaction between the projectile and target is more complicated than the situation of Eq. (1.1), where all the projectile charge density is assumed to be outside the target. In this connection, we explore the b range of the integral in Eq. (1.2), where $X(b)$ is making the transition from a small value (almost complete absorption) to near unity (almost no absorption).

More precisely, in Sec. II we consider the nucleon-nucleon interactions, and an explicit form will be deduced for the function $X(b)$. In Sec. III we will investigate the effect on $P_{\text{g.s.}\to\alpha}(b)$ of the overlapping of the projectile and target charge densities. We will then discuss in Sec. IV several prescriptions for the parameter $b_{\min}$ of Eq. (1.1), which will lead to the same calculated cross section as the more accurate Eq. (1.2).

II. NUCLEAR INTERACTION BETWEEN PROJECTILE AND TARGET

We discuss the nuclear interactions between the projectile and target nuclei in terms of the optical limit of the Glauber model [1], in which each projectile nucleon is treated as a grey disk. If a spherical projectile with nucleon number density $n_P(\mathbf{r})$ passes a spherical target with nucleon number density

[1] Transitions can also be induced in the projectile, because of the electromagnetic fields of the target. In this paper, we will assume that the projectile remains in its ground state throughout the collision.

$n_T(\mathbf{r})$ along a straight-line trajectory with impact parameter b, the probability of no nuclear interaction is given by

$$X(b) = e^{-\Lambda(b)}, \tag{2.1a}$$

with

$$\Lambda(b) \equiv \int_0^\infty q\ dq\ J_0(qb)\tilde{n}_P(q)\tilde{n}_T(q)\frac{f_{NN}(q)}{ik_{NN}}. \tag{2.1b}$$

The tilde represents a Fourier transform, so that

$$\tilde{n}_{P,T}(q) \equiv \frac{4\pi}{q}\int_0^\infty r\ dr\ \sin(qr)\, n_{P,T}(r), \tag{2.2}$$

and $f_{NN}(q)$ is related to the nucleon-nucleon scattering amplitude at relative momentum $\hbar k_{NN}$.

If the center-of-mass energy of the projectile and target nucleons is in the GeV region, as in relativistic Coulomb excitation, the spin-averaged nucleon-nucleon scattering amplitudes can be parametrized by (see, e.g., Ref. [2])

$$\frac{f_{ZZ}(q)}{ik_{ZZ}} \sim \frac{\sigma_{ZZ}}{4\pi}e^{-B_{ZZ}(\hbar q)^2},$$
$$\frac{f_{ZN}(q)}{ik_{ZN}} \sim \frac{\sigma_{ZN}}{4\pi}e^{-B_{ZN}(\hbar q)^2}.$$

We have distinguished here between identical nucleon parameters (designated ZZ) and nonidentical nucleon parameters (designated ZN). The numerical values of σ_{ZZ}, B_{ZZ}, σ_{ZN}, and B_{ZN}, which are functions of energy, were taken from Igo [2]. They are given in Table I.

The nucleon number densities required in Eq. (2.2) were taken from the IAEA compilation [3]. They are the results of Hartree-Fock-Bogoliubov calculations, whose parameters are fitted to measured nuclear masses. In a comparison involving 523 nuclei, these number densities agreed with measured radii within an rms error of 0.028 fm.

Bertulani *et al.* [4] used a similar approach to represent the effect of nuclear absorption in grazing collisions. Their analysis assumes that the nucleon-nucleon scattering amplitude is $\mathbf{q}$ independent. They do not distinguish between the interactions of identical and nonidentical nucleons. In different contexts, a similar approach has been developed by Benesh, Cook, and Vary [5] and by Kox *et al.* [6].

TABLE I. Parameters to determine the spin-averaged nucleon-nucleon scattering amplitudes, interpolated and extrapolated from figures given by Igo [2].

Bombarding energy (GeV per nucleon)	σ_{ZZ} (mb)	B_{ZZ} (GeV/c)$^{-2}$	σ_{ZN} (mb)	B_{ZN} (GeV/c)$^{-2}$
1	47.849	5.814	40.221	4.1
2	45.024	6.349	42.973	5.904
3	42.493	6.847	42.520	6.645
4	41.307	7.280	42.124	7.384
5	40.809	7.737	42.567	8.069

III. ELECTROMAGNETIC TRANSITION MATRIX ELEMENTS WITH OVERLAPPING CHARGE DISTRIBUTIONS

In the previous sections, we saw that at the bottom of the range of impact parameters there can be overlapping of the projectile and target charge distributions. We now consider whether this requires us to modify the standard analysis of relativistic Coulomb excitation, which is based on the assumption that the projectile and target charge distributions do not overlap.

A. Scalar and vector potentials

We orient our axes so that the projectile center moves with velocity $v\hat{\mathbf{z}}$ relative to the target center in their common $\hat{\mathbf{y}}$-$\hat{\mathbf{z}}$ plane. If (x, y, z, t) locate an event relative to the projectile, and (x', y', z', t') locate the same event relative to the target, then

$$x = x', \quad y = y' - b, \quad z = \gamma(z' - vt'),$$
$$t = \gamma\left(t' - \frac{v}{c^2}z'\right), \qquad \gamma \equiv \left(1 - \frac{v^2}{c^2}\right)^{-\frac{1}{2}}.$$

Suppose that the projectile charge density is static and spherically symmetric in its own rest frame, so that it can be written

$$\rho_P(x, y, z) = \rho_P(r), \quad r \equiv \sqrt{x^2 + y^2 + z^2}.$$

Then the scalar potential due to this charge distribution, as measured in the projectile rest frame, is given by

$$\phi_P(r) = \frac{4\pi}{r}\int_{s=0}^{r} s^2\rho_P(s)ds + 4\pi\int_{s=r}^{\infty} s\rho_P(s)ds. \tag{3.1}$$

It can be readily verified that this expression for $\phi_P(r)$ satisfies Poisson's equation for the specified projectile charge density:

$$\nabla_r^2\phi_P(r) = \frac{1}{r^2}\frac{d}{dr}r^2\frac{d}{dr}\phi_P(r) = -4\pi\rho_P(r).$$

The scalar potential measured by an observer at the target center can be determined from Eq. (3.1), since the scalar potential transforms as the 0 component of a Lorentz four-vector. This leads to

$$\phi'_P(x', y', z', t') = \gamma\phi_P(x, y, z, t)$$
$$= \frac{4\pi\gamma}{r}\int_{s=0}^{r} s^2\rho_P(s)ds + 4\pi\gamma\int_{s=r}^{\infty} s\rho_P(s)ds, \tag{3.2}$$

with $r = \sqrt{x'^2 + (y' - b)^2 + \gamma^2(z' - vt')^2}$. Note that there is no contribution in Eq. (3.2) from a projectile current density, as seen by a projectile-based observer. This would be the situation, for example, if the projectile were a doubly-closed-shell nucleus, in which every occupied shell-model state was matched by an occupied time-reversed state.

It is helpful to modify Eq. (3.2) by adding and subtracting the quantity $\frac{4\pi\gamma}{r}\int_r^\infty s^2\rho_P(s)ds$. This converts Eq. (3.2) into

$$\phi'_P(x',y',z',t') = \frac{4\pi\gamma}{r}\int_{s=0}^{\infty} s^2\rho_P(s)ds + 4\pi\gamma\int_{s=r}^{\infty}\left(s-\frac{s^2}{r}\right)\rho_P(s)ds. \quad (3.3a)$$

Since the total projectile charge is $Z_P e = \int_{s=0}^{\infty} 4\pi s^2\rho_P(s)ds$, this equation can be rewritten as

$$\phi'_P(x',y',z',t') = \frac{\gamma Z_P e}{\sqrt{x'^2+(y'-b)^2+\gamma^2(z'-vt')^2}} + 4\pi\gamma\int_{s=r}^{\infty}\left(s-\frac{s^2}{r}\right)\rho_P(s)ds. \quad (3.3b)$$

The first term on the right-hand sides of Eqs. (3.3a) and (3.3b) is the Lienard-Wiechert (LW) potential (see, e.g., Ref. [7]), which is the potential at (x',y',z',t') produced by a *point charge* $Z_P e$ at the projectile center, as measured by a target-based observer. The second term is a correction to the LW potential, needed when the projectile has charge that extends farther from the projectile center than the observation point (x',y',z',t'). In other words, this correction term is needed for points in space within the projectile charge distribution. It is seen that although the LW term involves only the total projectile charge $Z_P e$, the overlap correction term depends upon the radial shape of the projectile charge distribution.

The same Lorentz transformation that yields the scalar potential (3.2) yields the vector potential

$$\mathbf{A}'_P(\mathbf{r}',t') = \frac{v}{c}\phi'_P(\mathbf{r}',t')\hat{\mathbf{z}}. \quad (3.4)$$

B. Calculation of the transition charge density

Let us consider the specific case of a direct transition between the zero- and one-phonon states of the target giant dipole excitation. We will generate the transition charge and current densities with the Goldhaber-Teller model [8] of the giant dipole resonance (GDR), in which the target protons and neutrons oscillate relative to each other. For example, phonon excitations of the ^{40}Ca ground state can be constructed in which spherical clusters of 20 protons and 20 neutrons oscillate relative to each other, with the oscillation degree of freedom the vector $\mathbf{r}_{pn}$, drawn from the center of the neutron cluster to the center of the proton cluster (see Fig. 1). If the oscillations are small, the GDR potential can be expected to be approximately harmonic, and then the relative motion of the cluster centers would be governed by a harmonic oscillator wave function $\psi_m^{n,\ell}(\mathbf{r}_{pn})$. The ground state relative motion would be determined by $\psi_0^{0,0}(\mathbf{r}_{pn})$, and the ground state charge density would be

$$\rho_{\text{g.s.}}(\mathbf{r}') = e\int d^3r_{pn}\left[\psi_0^{0,0}(\mathbf{r}_{pn})\right]^*\psi_0^{0,0}(\mathbf{r}_{pn})G(|\mathbf{r}'-f\mathbf{r}_{pn}|). \quad (3.5a)$$

where $G(s)$ is the number density of the protons at a distance s from the center of the protons (see Fig. 1), and f is defined

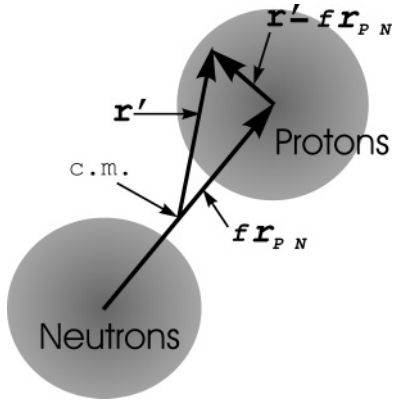

FIG. 1. Goldhaber-Teller picture of the GDR, with proton and neutron spheres oscillating relative to each other. The oscillation variable is $\mathbf{r}_{pn}$, the vector connecting the centers of the two spheres.

by

$$f \equiv \frac{N_T}{Z_T+N_T} = \frac{N_T}{A_T}, \quad (3.5b)$$

so that $f\mathbf{r}_{pn}$ is the vector connecting the target center of mass to the center of the target proton cluster, which we take to be an inert sphere. The transition charge density for the transition from the ground state to the GDR state with relative motion (n,ℓ,m) is given by

$$\rho_{\text{g.s.}\to(n,\ell,m)}(\mathbf{r}') = e\int d^3r_{pn}\left[\psi_m^{n,\ell}(\mathbf{r}_{pn})\right]^*\psi_0^{0,0}(\mathbf{r}_{pn}) \times G(|\mathbf{r}'-f\mathbf{r}_{pn}|). \quad (3.5c)$$

It will be sufficient for our purposes to consider the transition from the ground state to the mode

$$\psi_y \equiv \frac{1}{\sqrt{2}}\left[\psi_1^{0,1}+\psi_{-1}^{0,1}\right],$$

which is one quantum of oscillation in the $\hat{\mathbf{y}}$ direction. At high bombarding energy, this is the strongest direct transition. Because this state has a simple interpretation in a Cartesian representation, we rewrite Eq. (3.5a) and (3.5c) in terms of one-dimensional harmonic oscillator eigenstates:

$$\rho_{\text{g.s.}}(\mathbf{r}') = e\int dx_{pn}dy_{pn}dz_{pn}[\psi_0(x_{pn})]^2[\psi_0(y_{pn})]^2 \times[\psi_0(z_{pn})]^2G(|\mathbf{r}'-f\mathbf{r}_{pn}|), \quad (3.6a)$$

$$\rho_{\text{g.s.}\to y}(\mathbf{r}') = e\int dx_{pn}dy_{pn}dz_{pn}[\psi_0(x_{pn})]^2[\psi_1(y_{pn})\psi_0(y_{pn})] \times[\psi_0(z_{pn})]^2G(|\mathbf{r}'-f\mathbf{r}_{pn}|). \quad (3.6b)$$

The one-dimensional harmonic oscillator states needed here are

$$\psi_0(y_{pn}) = \left(\frac{\nu}{\pi}\right)^{\frac{1}{4}}e^{-\frac{1}{2}\nu y_{pn}^2},$$

$$\psi_1(y_{pn}) = \left(\frac{\nu}{\pi}\right)^{\frac{1}{4}}\sqrt{2\nu}\,y_{pn}e^{-\frac{1}{2}\nu y_{pn}^2} = -\sqrt{\frac{2}{\nu}}\frac{\partial}{\partial y_{pn}}\psi_0(y_{pn}),$$

so that

$$[\psi_1(y_{pn})\psi_0(y_{pn})] = -\sqrt{\frac{2}{\nu}}\psi_0(y_{pn})\frac{\partial}{\partial y_{pn}}\psi_0(y_{pn})$$

$$= -\frac{1}{\sqrt{2\nu}}\frac{\partial}{\partial y_{pn}}[\psi_0(y_{pn})]^2.$$

If we use this relation in Eq. (3.6b),

$$\rho_{\text{g.s.}\to y}(\mathbf{r}') = -\frac{e}{\sqrt{2\nu}}\int dx_{pn}dy_{pn}dz_{pn}[\psi_0(x_{pn})]^2$$

$$\times\frac{\partial}{\partial y_{pn}}[\psi_0(y_{pn})]^2[\psi_0(z_{pn})]^2 G(|\mathbf{r}' - f\mathbf{r}_{pn}|),$$

and integrate by parts, we get

$$\rho_{\text{g.s.}\to y}(\mathbf{r}') = +\frac{e}{\sqrt{2\nu}}\int dx_{pn}dy_{pn}dz_{pn}[\psi_0(x_{pn})]^2[\psi_0(y_{pn})]^2$$

$$\times[\psi_0(z_{pn})]^2\frac{\partial}{\partial y_{pn}}G(|\mathbf{r}' - f\mathbf{r}_{pn}|). \tag{3.7}$$

But

$$\frac{\partial}{\partial y_{pn}}G(|\mathbf{r}' - f\mathbf{r}_{pn}|) = -f\frac{\partial}{\partial y'}G(|\mathbf{r}' - f\mathbf{r}_{pn}|),$$

so that Eq. (3.7) becomes

$$\rho_{\text{g.s.}\to y}(\mathbf{r}') = -\frac{ef}{\sqrt{2\nu}}\frac{\partial}{\partial y'}\int dx_{pn}dy_{pn}dz_{pn}[\psi_0(x_{pn})]^2$$

$$\times[\psi_0(y_{pn})]^2[\psi_0(z_{pn})]^2 G(|\mathbf{r}' - f\mathbf{r}_{pn}|)$$

$$= -\frac{f}{\sqrt{2\nu}}\frac{\partial}{\partial y'}\rho_{\text{g.s.}}(\mathbf{r}') = -\frac{f}{\sqrt{2\nu}}\frac{y'}{r'}\frac{\partial}{\partial r'}\rho_{\text{g.s.}}(r')$$

$$= -\frac{f}{\sqrt{2\nu}}\sin(\theta')\sin(\phi')\frac{\partial}{\partial r'}\rho_{\text{g.s.}}(r'). \tag{3.8}$$

Thus the radial shape of the transition charge density is obtained from the *radial derivative of the target ground state charge density*. This result depends upon the interpretation of the GDR as a harmonic oscillation of proton and neutron spheres relative to each other, but it makes no assumption about the radial charge dependence of the proton sphere.

The occurrence of the derivative of the ground state radial density in expressions for transition densities is familiar from discussions of direct inelastic scattering to modes which are interpreted as small shape oscillations. An exhaustive discussion of this topic can be found, e.g., in Ch. 14 of Ref. [9]. These theories are based on expansions of the nuclear shape in powers of the small parameter describing the oscillation. We note that our derivation of Eq. (3.8) is not based on an expansion in powers of a small parameter. However, our use of harmonic oscillator wave functions in the derivation of Eq. (3.8) depended upon our assumption that the GDR potential is harmonic, which will generally be true only if the deviation from equilibrium is small.

The size parameter ν used in Eq. (3.6a) through (3.8) is given by $\nu = \mu\omega/\hbar$, where μ is the reduced mass for the neutron and proton spheres, and ω is the GDR oscillation frequency. We will use the generic formula [10]

$$\hbar\omega = 79\ A_T^{-\frac{1}{3}}, \tag{3.9}$$

where A_T is the target mass number.

C. Transition matrix element

Some of the basic formulas of the semiclassical approach to RCE are presented in the Appendix.

The time-dependent target transition matrix element is

$$V_{\text{g.s.}\to y}(t', b) = \int d^3r'\left[\rho_{\text{g.s.}\to y}(\mathbf{r}')\phi'_p(\mathbf{r}', t')\right.$$

$$\left. - \frac{1}{c}\mathbf{j}_{\text{g.s.}\to y}(\mathbf{r}')\cdot\mathbf{A}'_p(\mathbf{r}', t')\right]. \tag{3.10}$$

According to Eqs. (3.4) and (3.10), only the z component of the transition current density enters into the matrix element. This is zero for the matrix element connecting the zero-phonon state to the state with one phonon of oscillation in the $\hat{\mathbf{y}}$ direction. Thus, for this particular matrix element, we need only be concerned with the $\rho - \phi$ term in (3.10).

The partition of the scalar potential into LW and overlap terms carries over to the transition matrix element:

$$V_{\text{g.s.}\to y}(t', b) = V_{\text{LW}}(t') + V_{\text{overlap}}(t'), \tag{3.11a}$$

$$V_{\text{LW}}(t', b) = \int d^3r'\frac{\gamma Z_p e}{\sqrt{x'^2 + (y' - b)^2 + \gamma^2(z' - vt')^2}}$$

$$\times\rho_{\text{g.s.}\to y}(\mathbf{r}'), \tag{3.11b}$$

$$V_{\text{overlap}}(t', b) = 4\pi\gamma\int d^3r'\int_{s=r}^{\infty}\left(s - \frac{s^2}{r}\right)\rho_p(s)ds$$

$$\times\rho_{\text{g.s.}\to y}(\mathbf{r}'), \tag{3.11c}$$

with $r \equiv \sqrt{x'^2 + (y' - b)^2 + \gamma^2(z' - vt')^2}$. For the purposes of calculation, it is convenient to define a function $F(r)$ by

$$F(r) \equiv 4\pi\gamma\int_{s=r}^{\infty} s(s - r)\rho_p(s)ds. \tag{3.12}$$

Then $V_{\text{LW}}(t')$ and $V_{\text{overlap}}(t')$ can be written more compactly as

$$V_{\text{LW}}(t') = \int d^3r'\frac{\rho_{\text{g.s.}\to y}(\mathbf{r}')}{r}F(0), \tag{3.13a}$$

$$V_{\text{overlap}}(t') = -\int d^3r'\frac{\rho_{\text{g.s.}\to y}(\mathbf{r}')}{r}F(r), \tag{3.13b}$$

with $r \equiv \sqrt{x'^2 + (y' - b)^2 + \gamma^2(z' - vt')^2}$. Once $\rho_p(s)$, the radial form of the projectile proton density distribution, has been chosen, $F(r)$ is calculated using Eq. (3.12), and then it is used in the numerical evaluation of the integrals (3.13a) and (3.13b).

D. Cross sections

Up to bombarding energies of about 5 GeV per nucleon, first-order time-dependent perturbation theory accounts for almost all of the population of the state with one phonon of

TABLE II. $\sigma_{\rm LW}$ and $\sigma_{\rm overlap}$, defined in Eq. (3.14), for ^{16}O and ^{208}Pb projectiles bombarding ^{74}Ge and ^{202}Hg targets, at 2 GeV per nucleon.

Projectile	^{74}Ge target		^{202}Hg target	
	$\sigma_{\rm LW}$ (barns)	$\sigma_{\rm overlap}$ (barns)	$\sigma_{\rm LW}$ (barns)	$\sigma_{\rm overlap}$ (barns)
^{16}O	1.9×10^{-2}	-9.3×10^{-5}	7.3×10^{-2}	-9.9×10^{-5}
^{208}Pb	1.3	-3.5×10^{-4}	5.8	-3.5×10^{-4}

oscillation in the $\hat{\mathbf{y}}$ direction (see, e.g., [11]). This leads to

$$P_{\rm g.s.\to y}(b) = \left| \int_{-\infty}^{\infty} \frac{dt'}{\hbar} e^{i\omega t'} V_{\rm g.s.\to y}(t', b) \right|^2 \equiv |\tilde{V}_{\rm g.s.\to y}(\omega, b)|^2,$$

where $\tilde{V}_{\rm g.s.\to y}(\omega, b)$ is the "on-shell" Fourier component of $V_{\rm g.s.\to y}(t', b)$ (see Appendix). Using Eq. (1.2), we can write[2]

$$\begin{aligned}
\sigma &= \int bdb |\tilde{V}_{\rm g.s.\to y}(\omega, b)|^2 X(b) \\
&= \int bdb |\tilde{V}_{\rm LW}(\omega, b) + \tilde{V}_{\rm overlap}(\omega, b)|^2 X(b) \\
&= \int bdb (\tilde{V}_{\rm LW}(\omega, b))^2 X(b) \\
&\quad + \int bdb \tilde{V}_{\rm overlap}(\omega, b) \times (2\tilde{V}_{\rm LW}(\omega, b) \\
&\quad + \tilde{V}_{\rm overlap}(\omega, b)) X(b) \\
&= \sigma_{\rm LW} + \sigma_{\rm overlap}. \qquad (3.14)
\end{aligned}$$

Here $\sigma_{\rm LW}$ is the cross section that would have been calculated had the Lienard-Wiechert potential been used *everywhere*, even in the overlap region, and $\sigma_{\rm overlap}$ is the correction that must be applied due to the inadequacy of the Lienard-Wiechert potential.

Application of the Winther-Alder [12] general formula, Eq. (A1), to $\tilde{V}_{\rm LW}(\omega, b)$ gives

$$\begin{aligned}
\tilde{V}_{\rm LW}(\omega, b) = &-\frac{\pi c Z_P e f}{\hbar \gamma v^2} \sqrt{\frac{32}{\nu}} K_1\left(\frac{\omega b}{\gamma v}\right) \\
&\times \int_0^{\infty} r'^2 dr' j_1\left(\frac{\omega}{c} r'\right) \frac{\partial \rho_{\rm g.s.}(r')}{\partial r'}. \qquad (3.15)
\end{aligned}$$

We can use this in Eq. (3.14), but $\tilde{V}_{\rm overlap}(\omega, b)$ must be evaluated numerically, as must the b integral in $\sigma_{\rm overlap}$. The latter is simplified by the fact that the effective b range is finite. It is limited from below by the vanishing of $X(b)$ and from above by the vanishing of $\tilde{V}_{\rm overlap}(\omega, b)$, since large b implies small overlap.

Table II shows a comparison of $\sigma_{\rm LW}$ and $\sigma_{\rm overlap}$ for ^{16}O and ^{208}Pb projectiles bombarding ^{74}Ge and ^{202}Hg targets at 2 GeV per nucleon. It is seen that $\sigma_{\rm LW}$ is very much larger when ^{208}Pb is the projectile and ^{202}Hg is the target. This is because *all* the projectile and target charges contribute to the LW cross section. However, the amount of overlap charge is approximately the same in all four cases, so that the four overlap corrections are of the same order of magnitude. Another feature that suppresses the overlap correction in the heavier systems is their greater neutron/proton ratio. The extra neutrons contribute to the absorption, but not to the electromagnetic interaction.

Although $\sigma_{\rm overlap}$ is a greater fraction of $\sigma_{\rm LW}$ in lighter systems than in heavier systems, we can see from Table II that $\sigma_{\rm overlap}$ is *always* very small compared to $\sigma_{\rm LW}$. Thus we can safely ignore $\sigma_{\rm overlap}$, and use $\sigma_{\rm LW}$ alone to account for experimental data.

IV. PROJECTILE AND TARGET DEPENDENCE OF $b_{\rm min}$

Suppose that $X(b)$ makes a sharp transition from 0 to 1 as b crosses a particular value $b_{\rm min}$. Then Eq. (3.14) yields

$$\sigma_{\rm LW} = \int_{b=b_{\rm min}}^{\infty} bdb (\tilde{V}_{\rm LW}(\omega, b))^2 \qquad (4.1)$$

Application of Eq. (A1) through (A4) gives

$$\begin{aligned}
\sigma_{\rm LW} = \pi b_{\rm min}^2 &\left[\left(K_2\left(\frac{\omega b_{\rm min}}{\gamma v}\right)\right)^2 - \left(K_1\left(\frac{\omega b_{\rm min}}{\gamma v}\right)\right)^2 \right. \\
&\left. - 2\left(\frac{\gamma v}{\omega b_{\rm min}}\right)^2 K_2\left(\frac{\omega b_{\rm min}}{\gamma v}\right) K_1\left(\frac{\omega b_{\rm min}}{\gamma v}\right) \right] \\
&\times \left(\frac{\pi c Z_P e f}{\hbar \gamma v^2} \sqrt{\frac{32}{\nu}} \int_0^{\infty} r'^2 dr' j_1\left(\frac{\omega}{c} r'\right) \frac{\partial \rho_{\rm g.s.}(r')}{\partial r'} \right)^2. \qquad (4.2)
\end{aligned}$$

It would be advantageous to have a prescription for $b_{\rm min}$ such that the entire expression (3.14) for the cross section would be given by the explicit formula (4.2). Equivalently, we seek a formula for $b_{\rm min}$ that satisfies[3]

$$\int_{b=0}^{\infty} bdb\, [\tilde{V}_{\rm LW}(\omega, b)^2] X(b) = \int_{b=b_{\rm min}}^{\infty} bdb\, [\tilde{V}_{\rm LW}(\omega, b)^2].$$

Since all the b dependence of $\tilde{V}_{\rm LW}(\omega, b)$ is contained in $K_1\left(\frac{\omega b_{\rm min}}{\gamma v}\right)$, we can write this equation more explicitly as

$$\int_{b=0}^{\infty} bdb \left(K_1\left(\frac{\omega b}{\gamma v}\right)\right)^2 X(b) = \int_{b=b_{\rm min}}^{\infty} bdb \left(K_1\left(\frac{\omega b}{\gamma v}\right)\right)^2. \qquad (4.3)$$

We could use $b_{\rm min}$ defined in this way in Eq. (4.2), thus incorporating the effect of nuclear interactions during grazing collisions of the projectile and target.

Since the left-hand side of Eq. (4.3) must be evaluated numerically, we cannot produce a closed formula for $b_{\rm min}$.

[2] These matrix elements are real.

[3] Bertulani *et al.* [4] use the symbol $b_{\rm sharp}$ to represent this quantity.

However, we can numerically evaluate Eq. (4.3) for a variety of projectiles, targets, and bombarding energies, and then look for regularities that could guide our choice of $b_{\min}$ in any particular situation. To carry out this program, we selected as projectiles the nuclei ^{16}O, ^{40}Ca, ^{120}Sn, and ^{208}Pb, and as targets the nuclei ^{16}O, ^{32}S, ^{52}Cr, ^{74}Ge, ^{90}Zr, ^{114}Cd, ^{138}Ba, ^{158}Gd, ^{180}Hf, and ^{202}Hg. The GDR oscillation frequencies were given by Eq. (3.9). For each projectile-target combination, we varied the bombarding energy from 1 to 5 GeV per nucleon, in steps of 1 GeV per nucleon, and used Eq. (4.3) to calculate the appropriate value of $b_{\min}$.

In the limit of very large nucleon-nucleon interaction cross sections, we would expect $b_{\min}$ to be of the order of $R_P + R_T$, or perhaps somewhat larger if the finite range of the nucleon-nucleon interaction is included. This would lead to an expression for $b_{\min}$ proportional to $A_P^{1/3} + A_T^{1/3}$. However, a more realistic nucleon-nucleon interaction would allow the projectile and target densities to overlap slightly without nuclear interaction, which would lead to a smaller value of $b_{\min}$. If the projectile and/or the target have large radii, even a small amount of penetration implies a large overlap volume and thus a large nuclear interaction probability. Thus, the downward correction to an $A_P^{1/3} + A_T^{1/3}$ term would be expected to decrease as the size of the colliding nuclei increases. The simplest way to incorporate these trends into a formula is to seek parameters λ, μ such that

$$b_{\min} \sim \lambda\left(A_P^{1/3} + A_T^{1/3}\right) - \mu\left(A_P^{-1/3} + A_T^{-1/3}\right). \qquad (4.4)$$

This is the form used by Benesh *et al.* [5] in their analysis of the total reaction cross section for colliding nuclei. We have chosen λ and μ to produce the best fit, in a least-squares sense to the 200 ($4 \times 10 \times 5$) projectile-target-energy combinations for which we have numerically calculated $b_{\min}$ using Eq. (4.3). The result is

$$\lambda = 1.3115 \text{ fm}, \qquad \mu = 1.0509 \text{ fm}.$$

If these paramaters are used in Eq. (4.4), the calculated values of $b_{\min}$ are reproduced with an r.m.s. error of 0.0248 fm per point. A graphical comparison is shown in Fig. 2. The continuous lines are plots of Eq. (4.4) for our four projectiles, and the plotted points refer to our numerical calculations of $b_{\min}$ for our ten targets at bombarding energies of 1 and 5 GeV per nucleon. It is seen that Eq. (4.4), with the parameters given above, provides an excellent representation of the $b_{\min}$ values numerically calculated from Eq. (4.3).

Another study [6] of nucleus-nucleus reaction cross sections adopted a form equivalent to

$$b_{\min} \sim \lambda\left(A_P^{1/3} + A_T^{1/3}\right) + \mu\frac{A_P^{1/3} \times A_T^{1/3}}{A_P^{1/3} + A_T^{1/3}} - c. \qquad (4.5)$$

This equation contains three adjustable parameters, λ, μ, and c. A least-square-deviation fit to our 200 values of $b_{\min}$ yields

$$\lambda = 1.3338 \text{ fm}, \qquad \mu = 0.1652 \text{ fm}, \qquad c = 1.0667 \text{ fm},$$

with an r.m.s error of 0.0382 fm per point. We see that the form (4.5) with three free parameters does not produce as good an overall fit as the form (4.4), which has only two free parameters. We conclude that Eq. (4.4) gives the most effective and economical representation of the dependence of $b_{\min}$ on projectile and target mass numbers.

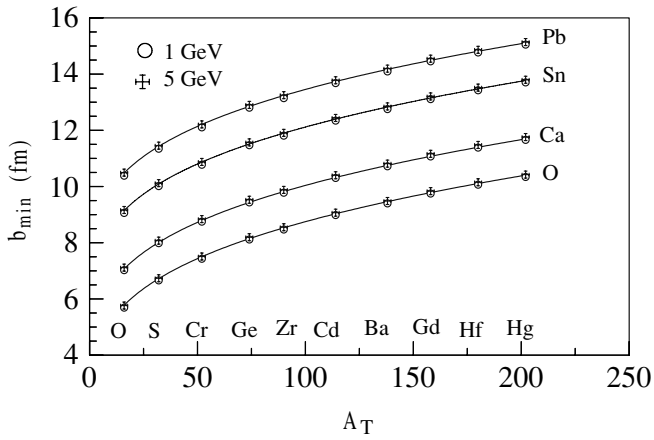

FIG. 2. Circles correspond to $b_{\min}$ values calculated using Eq. (4.3), when the bombarding energy is 1 GeV per nucleon. Crosses are the same, but for a bombarding energy of 5 GeV per nucleon. Continuous lines were calculated using Eq. (4.4), with $\lambda = 1.3115$ fm and $\mu = 1.0509$ fm.

The $b_{\min}$ values given by Eqs. (4.4) or (4.5) yield very nearly the same Coulomb excitation (CEX) cross sections when substituted into Eq. (4.2). The differences are less than 1% for all cases except for 1 GeV per nucleon ^{16}O projectiles on a ^{16}O target, where the difference is 2%. These differences are probably small compared to the errors associated with the use of first-order time-dependent perturbation theory.

V. DISCUSSION

All the calculations presented so far have referred to $\mu = 1$ transitions, i.e., transitions in which the transfer of the $\hat{\mathbf{z}}$ component of angular momentum is $\pm\hbar$. These are the dominant transitions in RCE. Indeed, in the Weizsäcker-Williams [13] approach to RCE, these are the *only* transitions considered. Nevertheless, transitions with $\mu \neq 1$ are possible, and it is of some interest to know how a change in μ would affect $b_{\min}$. This can be answered simply by replacing K_1 in Eq. (4.3) by K_μ. In the vicinity of $b \sim b_{\min}$, the argument of $K_\mu\left(\frac{\omega b_{\min}}{\gamma v}\right)$ is small, which implies that K_μ is proportional to $b^{-\mu}$. Thus K_μ falls more sharply with increasing b as μ increases, and this has the consequence that $b_{\min}$ calculated from Eq. (4.3) will decrease as μ increases. Another way to reach this conclusion is to think about the μ component of the transition charge density. As μ increases, the centrifugal potential will keep the transition charge density farther away from the $\hat{\mathbf{z}}$ axis. Thus absorption, which occurs close to the $\hat{\mathbf{z}}$ axis, will have less effect on high μ transitions. Since it is absorption that gives rise to a minimum effective value of b, less absorption will mean a smaller value of $b_{\min}$.

We have done calculations for $\mu = 2$ and found a decrease in $b_{\min}$, compared to the $\mu = 1$ values presented in the last section, by about 0.05 fm when the projectile is ^{208}Pb. For the range of targets and bombarding energies we have studied, this decrease in $b_{\min}$ is equivalent to an increase in CEX

cross section of about 0.7% to 1.5%. This difference is small enough to be ignored in practical calculations. If the projectile is ^{16}O, the corresponding error in $b_{\min}$ is about 0.1 fm, which is equivalent to errors of about 1.5% to 7% in CEX cross sections. Thus, for lighter projectiles, and in situations in which $\mu > 1$ transitions are expected to be important, the values of $b_{\min}$ calculated with Eqs. (4.4) and (4.5) should be interpreted only as upper limits.

To do a calculation that accurately includes the effect of absorption when several values of μ are important, it is necessary to give up the picture implied by Eq. (1.2), in which absorptive processes occur independently of the Coulomb excitation. Rather, the coupled equations that are used to calculate the transition amplitude would have to include absorptive processes along with electromagnetic processes. This would be analagous to the way that optical model analyses of inelastic scattering employ an imaginary potential to simulate absorption into other channels in the calculation of the inelastic scattering amplitude.

APPENDIX: SOME BASIC FORMULAS OF THE SEMICLASSICAL APPROACH TO RELATIVISTIC COULOMB EXCITATION

The Fourier transform of the matrix element for the transfer of angular momenta (λ, μ) in the target transition $\phi_\alpha \to \phi_\beta$, due to the time-dependent electromagnetic field of a spherically symmetric projectile moving with speed v along a trajectory with impact parameter b is

$$V_{\beta\alpha}(\omega, b) \equiv \int_{-\infty}^{\infty} \frac{dt'}{\hbar} V_{\beta\alpha}(t', b) = \frac{2Z_P e}{\hbar v} e^{-i\phi_b} \left[\mathcal{G}_{\lambda,\mu} \int d^3r' \left(\rho_{\beta\alpha}(\mathbf{r}') - \frac{v}{c^2} \hat{\mathbf{z}} \cdot \mathbf{j}_{\beta\alpha}(\mathbf{r}') \right) \times j_\lambda \left(\frac{|\omega|}{c} r' \right) Y_\mu^\lambda(\hat{r}') \right] K_\mu \left(\frac{|\omega| b}{\gamma v} \right). \quad \text{(A1)}$$

Here $\rho_{\beta\alpha}(\mathbf{r}')$ and $\mathbf{j}_{\beta\alpha}(\mathbf{r}')$ are the target charge and current transition charge densities for the states $\phi_\alpha \to \phi_\beta$, and K_μ is a modified Bessel function. The coefficients $\mathcal{G}_{\lambda,\mu}$ are defined by

$$\mathcal{G}_{\lambda,\mu} \equiv \frac{i^{\lambda+\mu}}{(2\gamma)^\mu} \left(\frac{|\omega|}{\omega} \right)^{\lambda-\mu} \sqrt{4\pi(2\lambda+1)(\lambda-\mu)!(\lambda+\mu)!} \times \sum_n \frac{1}{(2\gamma)^{2n}(n+\mu)!n!(\lambda-\mu-2n)!}. \quad \text{(A2)}$$

This expression assumes there is no overlap between projectile and target charge. The *time reversal* phase convention is used, so that the spherical harmonics Y_m^ℓ has an extra factor of i^ℓ compared to a Condon-Shortley spherical harmonic.

If it is assumed that no contribution to RCE occurs from $b < b_{\min}$ and no nuclear interactions occur for $b > b_{\min}$, then the first-order time-dependent perturbation theory approximation for the cross section for the RCE population of a state ϕ_μ^λ in an even-even nucleus is

$$\sigma = 2\pi \int_{b=b_{\min}}^{\infty} b db |V_{\beta\alpha}(\omega, b)|^2. \quad \text{(A3)}$$

The value of ω to be used here is $\frac{1}{\hbar}$ times the excitation energy of ϕ_μ^λ. This is sometimes referred to as the "on-shell" ω value. For the calculations in this paper, the excited state corresponds to a one-phonon excitation of the GDR, and thus the on-shell value of ω is given by Eq. (3.9). Because all the b dependence of $V_{\beta\alpha}(\omega, b)$ is contained in the factor $K_\mu \left(\frac{|\omega| b}{\gamma v} \right)$, the b integral in Eq. (A3) can be performed exactly, with the help of

$$\int_\xi^\infty (K_\mu(x))^2 x dx = \frac{\xi^2}{2} \left[(K_{\mu+1}(\xi))^2 - (K_\mu(\xi))^2 - \frac{2\mu}{\xi} (K_{\mu+1}(\xi) K_\mu(\xi)) \right]. \quad \text{(A4)}$$

[1] R. J. Glauber, *High-Energy Collisions Theory, Lectures in Theoretical Physics* (Interscience, New York, 1959), p. 315.
[2] G. Igo, AIP Conf. Proc. No. 26, edited by E. Nagle, A. S. Goldhaber, C. K. Hargrave, R. L. Burman, and B. G. Storms (AIP, New York, 1975), p. 63.
[3] S. Goriely, M. Samyn, and M. Pearson, HFB prediction of the nucleon density distributions, 2002, www-nds.iaea.org/RIPL-2/masses
[4] C. A. Bertulani, L. F. Canto, M. S. Hussein, and A. F. R. de Toledo Piza, Phys. Rev. C **53**, 334 (1996).
[5] C. J. Benesh, B. C. Cook, and J. P. Vary, Phys. Rev. C **40**, 1198 (1989).
[6] S. Kox *et al.*, Phys. Rev. C **35**, 1678 (1987).
[7] J. D. Jackson, *Classical Electrodynamics* (Wiley, New York, 1975).
[8] M. Goldhaber and E. Teller, Phys. Rev. **74**, 1046 (1948).
[9] G. R. Satchler, *Direct Nuclear Reactions* (Clarendon Press, Oxford, 1983).
[10] A. Bohr and B. R. Mottelson, *Nuclear Structure* (Benjamin, New York, 1975), Vol. II.
[11] B. F. Bayman and F. Zardi, Phys. Rev. C **68**, 014905 (2003).
[12] A. Winther and K. Alder, Nucl. Phys. **A319**, 518 (1979).
[13] C. F. Weizsäcker, Z. Phys. **88**, 612 (1934); E. J. Williams, Phys. Rev. **45**, 729 (1935).